Isentropic Scaling Law for Implosions of Solid Spherical Targets

Takashi SHIROTO*

Department of Physics, Nagoya University, Nagoya 464-8602, Japan

(Received 16 November 2025 / Accepted 5 January 2026)

In this study, an isentropic scaling law is developed for direct-drive implosions of solid spherical targets—a setup frequently employed in Fast Ignition Realization Experiments—in order to estimate densities at maximum compression. Adiabatic theories usually cannot explain shock-driven compression due to entropy production; however, differences among similar implosion scenarios can be approximated by isentropic laws. Numerous one-dimensional implosion simulations support for the proposed isentropic scaling law, especially regarding the relationship between confinement time and density at maximum compression.

Keywords: implosion, hydrodynamics, fast ignition, theoretical model

DOI: 10.1585/pfr.21.1404018

1. Introduction

In the recent Fast Ignition Realization Experiment (FIREX) project, solid spherical targets have been used instead of conventional shell targets to achieve stable hydrodynamic implosions and to focus on laser-plasma interaction studies driven by short-pulse lasers [1–5]. The direct-drive implosions of shell targets are vulnerable to hydrodynamic instabilities, such as the Rayleigh-Taylor instability, due to their high in-flight aspect ratio (IFAR). In contrast, the IFAR is unity for solid spheres, enabling hydrodynamically stable implosions. However, for central ignition schemes, the formation of a central hot spark is required, which makes the use of solid spheres infeasible. In fast ignition, a hot spark is instantaneously created by applying short-pulse lasers at maximum compression. This suggests that the solid spherical target is a promising candidate for fast ignition. Kidder has theoretically proposed isentropic implosions with solid spheres [6]. Since real plasmas exhibit more complex behavior than an ideal gas due to quantum effects, practical target designs employing multi-pulse drivers have been investigated to mitigate shock heating [7–9].

According to the numerical predictions, multi-step pulse lasers can create higher density cores than Gaussian pulses. However, at kJ-class laser facilities such as Gekko XII, the lifetime of the imploded core is extremely short, making experimental observation challenging. The monochromatic X-ray backlighting technique is the most reliable method for density diagnostics [2]. It requires precise synchronization between the long-pulse lasers used for implosion and the short-pulse lasers used for backlighting. Imploded cores that are optimized for kJ-class lasers survive for at most around 100 picoseconds. The success of measurements at maximum compression depends on random factors arising from jitter caused by electrical noise.

As an alternative approach, an isentropic scaling law was developed to estimate the density at maximum compression and was benchmarked using a number of one-dimensional implosion simulations. In principle, shock heating results in entropy production, so implosion dynamics cannot be described using only adiabatic fluid equations. This paper is based on the strong assumption that an adiabatic theory can explain the differences between similar implosion scenarios, even when shock waves are present. The structure of this paper is as follows: Sec. 2 derives scaling laws based on adiabatic hydrodynamics under the ideal gas assumption. Section 3 presents the results of one-dimensional implosion simulations using three-step pulse lasers to verify the isentropic scaling law. Section 4 discusses the limitations of the isentropic scaling proposed in this study. Section 5 presents the conclusions of this study.

2. Scaling Law

As mentioned in the previous section, this study assumes that differences among similar implosion scenarios behave adiabatically. The radius at maximum compression is defined as $R_{\max}$, and various parameters relevant to implosion dynamics are expressed as polynomials of $R_{\max}$. $R_{\max}$ is defined as the outermost radius at which the density is greater than $\rho_{\max}/e$, where $\rho_{\max}$ is the maximum density and e is the Euler's number. When the peak power is fixed, the maximum laser intensity, $I_{\max}$, is given by the following relation:

$$I_{\max} \propto {R_{\max}}^{-2}. \tag{1}$$

Here, $R_{\max}$ does not have to be identical to the radius at the

*Corresponding author's e-mail: shiroto.takashi.v2@f.mail.nagoya-u.ac.jp

critical density. However, this theory is based on the assumption that R_{max} is correlated with the critical surface. Since pressure is known to be proportional to the two-thirds power of laser intensity, the pressure at maximum compression (p_{max}) can be derived as follows:

$$p_{max} \propto {I_{max}}^{\frac{2}{3}} \propto {R_{max}}^{-\frac{4}{3}}. \quad (2)$$

Additionally, the density at maximum compression is related to p_{max} through isentropic processes:

$$\rho_{max} \propto {p_{max}}^{\frac{1}{\gamma}} \propto {R_{max}}^{-\frac{4}{3\gamma}}, \quad (3)$$

where γ is the specific heat ratio. Using the adiabatic hydrodynamics, the sound speed c_s is given as follows:

$$c_s \propto \sqrt{p_{max}/\rho_{max}} \propto {R_{max}}^{-\frac{2(\gamma-1)}{3\gamma}}. \quad (4)$$

The time scale for imploded cores to expand after maximum compression is referred to as the confinement time, τ:

$$\tau = R_{max}/c_s \propto {R_{max}}^{\frac{5\gamma-2}{3\gamma}}. \quad (5)$$

τ is the time duration during which the instantaneous maximum density is greater than ρ_{max}/e. One important result is that the density at maximum compression, ρ_{max}, can be estimated from the confinement time, τ:

$$\rho_{max} \propto \tau^{\frac{4}{5\gamma-2}}. \quad (6)$$

The rest of this paper assumes $\gamma = 5/3$.

3. Numerical Experiments

This section presents a series of one-dimensional implosion simulations to verify the isentropic scaling laws derived in Sec. 2. The targets are solid polystyrene spheres with diameters of 200, 250, 300, 350, and 400 μm. The three-step pulses used in this paper can be expressed as follows:

$$\begin{aligned} P(t) = {} & P_1 f(t;0.25) + (P_2 - P_1) f(t;T_1) \\ & + (P_3 - P_2) f(t;T_2) \end{aligned}, \quad (7)$$

where P_1, P_2, and P_3 represent the power at each stage of a three-step pulse, and the switching times of each stage are denoted by T_1 and T_2. The total pulse duration is $T_3 = 5$ [ns]. The function $f(t;T)$ is introduced to switch each stage, with a rise time of 0.125 ns, and is expressed as follows:

$$f(t;T) = \frac{\mathrm{erf}\left(\frac{t-T}{\sqrt{2}\sigma}\right)+1}{2}, \quad \sigma = \frac{0.125}{2\sqrt{2\ln 2}}\,[\mathrm{ns}]. \quad (8)$$

The parameters required to determine pulse shapes are denoted in Tables 1 and 2.

Additionally, to examine the robustness of the scaling law against uncertainties in laser intensity, numerical experiments were conducted in which the intensity of each step was perturbed by ± 10%. Thus, seven implosion calculations were performed for each target, including the optimized pulse shape. Furthermore, since laser absorption is significantly related to the laser wavelength, 527-nm and 351-nm lasers are employed to examine the impact of the laser wavelength on the scaling law. The former is referred to as 2ω, and the latter is referred to as 3ω. A total of 70 implosion simulations were performed and compared with the scaling law.

Table 1. The diameters of solid spheres and the corresponding three-step pulse lasers (2ω).

d [μm]	P_1 [TW]	P_2 [TW]	P_3 [TW]	T_1 [ns]	T_2 [ns]
200	8.0×10^{-3}	1.0×10^{-1}	3.0	3.5	4.6
250	2.4×10^{-2}	2.4×10^{-1}	2.6	3.5	4.5
300	4.7×10^{-2}	3.0×10^{-1}	2.0	3.5	4.5
350	8.5×10^{-2}	4.0×10^{-1}	2.0	3.6	4.6
400	1.4×10^{-1}	4.5×10^{-1}	2.0	3.5	4.6

Table 2. The diameters of solid spheres and the corresponding three-step pulse lasers (3ω).

d [μm]	P_1 [TW]	P_2 [TW]	P_3 [TW]	T_1 [ns]	T_2 [ns]
200	6.5×10^{-3}	7.0×10^{-2}	2.0	3.5	4.6
250	1.8×10^{-2}	1.4×10^{-1}	2.0	3.5	4.6
300	4.0×10^{-2}	2.3×10^{-1}	2.0	3.5	4.6
350	7.5×10^{-2}	4.0×10^{-1}	2.0	3.6	4.6
400	1.3×10^{-1}	4.5×10^{-1}	2.0	3.5	4.6

These numerical experiments were carried out using the radiation hydrodynamics code PheNiX [10]. PheNiX solves single-fluid, two-temperature hydrodynamic equations that include energy source terms. These terms consist of laser absorption, thermal conduction, radiative transfer, and collisional relaxation. The laser absorption is calculated using one-dimensional ray-tracing and the opacity of inverse-bremsstrahlung. The refraction and wave nature of lasers are neglected. The thermal conduction is approximated in the flux limited diffusion form with conductivities of Spitzer-Härm and a flux limiter of 0.06 [11]. The radiative transfer in multi-group diffusion form is solved with a variable Eddington factor proposed by Minerbo [12]. The emissivity and opacity are calculated using the average ion model and the screened hydrogenic model [13]. The free energy is estimated by Cowan model for ions and Thomas-Fermi model for electrons, resulting in tabulated equations of state (EOS) [14, 15]. The computational domain in radial direction is 500 μm divided into 1,024 cells.

This section compares the scaling laws (Eqs. (2), (3), (5), and (6)) with the results of numerical experiments. The hydrodynamic quantities are defined based on the simulation results. ρ_{max} and p_{max} are the maximum local density and pressure values, respectively.

Figures 1–3 show a comparison of the three independent scaling laws (Eqs. (2), (3), and (5)) with the simulation data. These scaling laws accurately reproduce the results of the one-dimensional implosion simulations. While agreement with a single formula could be coincidental, the consistency observed in density, pressure, and confinement time indicates that the assumptions of the scaling laws are reasonable. However, since the implosion dynamics in each case cannot

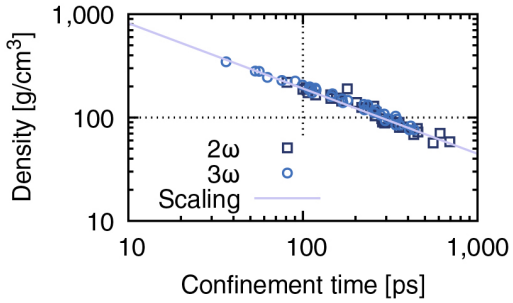

Fig. 1. The relation between the radius and density at maximum compression.

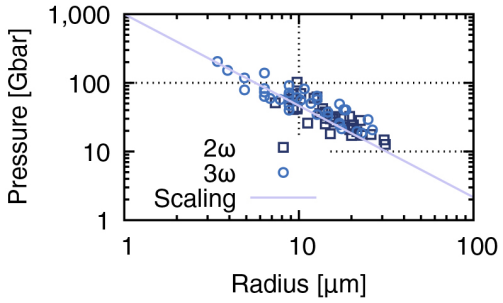

Fig. 2. The relation between the radius and pressure at maximum compression.

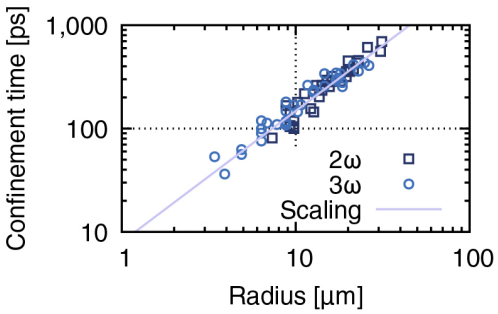

Fig. 3. The relation between the radius at maximum compression and the confinement time.

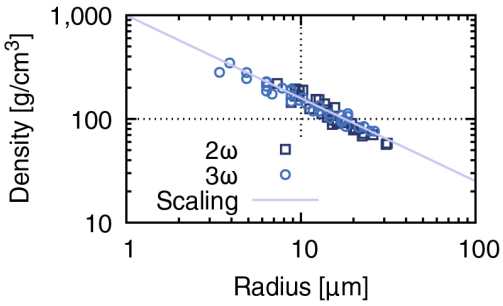

Fig. 4. The relation between the confinement time and the density at maximum compression.

be approximated adiabatically due to the effects of shock waves, thermal conduction, and radiative transfer, this outcome should not be considered self-evident.

Because the critical density is affected by the laser wavelength, it is difficult to reproduce both 2ω and 3ω implosions with a single scaling law. However, the numerical experiments suggest the proposed scaling law reproduces both types of implosions. Although the achievable density and pressure depend heavily on the laser wavelength, the data simply fall within different regions of the scaling law.

Furthermore, Fig. 4 shows that the relationship between confinement time and density at maximum compression (Eq. (6)) accurately explains the numerical results. Because expansion after maximum compression is a purely hydrodynamic process, it allows for more accurate predictions than other scaling laws.

It is challenging for the monochromatic X-ray backlight method to measure the core at maximum compression, particularly when the confinement time is less than 100 ps. The proposed scaling law has the possibility to estimate the density of such a short-lifetime core. While capturing the instant of maximum compression is difficult with monochromatic X-ray backlight measurements, taking multiple measurements around this moment is possible. Calculating the confinement time from these snapshots makes it possible to estimate the density at maximum compression. Note that this method only allows estimation of relative values, compared to other cases, and absolute density measurement is impossible. In other words, density estimation using this scaling law is only feasible if absolute density values can be measured using another method.

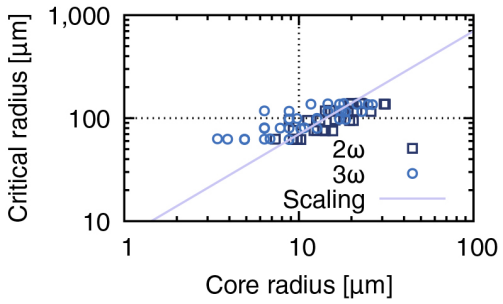

Fig. 5. The relation between the core radius at maximum compression and the minimum radius of critical surface.

4. Limitations of the Isentropic Scaling

Finally, some limitations of the proposed theory are mentioned here. The derivation of the proposed scaling is based on the assumption that the radius of the critical surface is proportional to the core radius at maximum compression. Figure 5 quantifies this correlation explicitly using the simulation data. This result suggests that the radii of the critical surface and the core do not have strong correlation, and this is the reason of relatively large errors in Eqs. (3)–(5).

The validity of the proposed theory strongly depends on the EOS. Figure 6 shows a comparison between the adiabatic indices of realistic plasma (γ') and ideal gas (γ). The area enclosed by the dotted line is of interest in the implosion dynamics, where the ideal gas model adequately explains the proposed scaling. However, the validity of the isentropic scaling law is confirmed only for the polystyrene. In order to apply the proposed theory to other materials, one must check

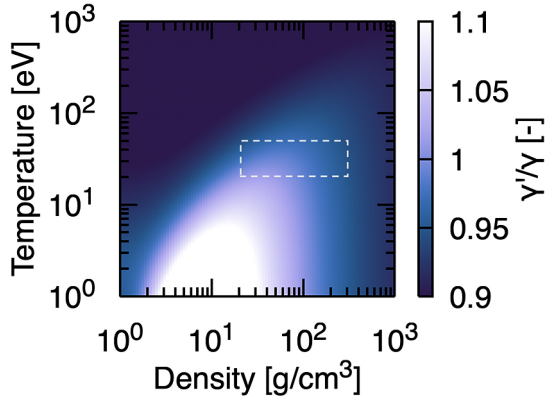

Fig. 6. The EOS table of polystyrene employed in this study.

EOS tables to determine the appropriate adiabatic indices.

The proposed theory assumes that the differences among implosion scenarios are isentropic, although variations in shock timing, absorption efficiency, thermal conduction, and radiation losses are well-known entropy sources in implosions. The proposed theory is expected to be valid for cases with nearly the same adiabat, which is the ratio between the hydrodynamic and Fermi pressures. Therefore, the differences between single-step and multi-step compressions cannot be explained by the isentropic scaling law.

It should be noted that the scaling law has only been verified in one-dimensional simulations in this study. For example, if the core undergoes significant deformation due to hydrodynamic instabilities, one cannot expect points to be plotted on the same line as in the case of symmetric implosions. Therefore, the scaling law should only be applied to cases where spherical symmetry is not a significant concern.

5. Conclusion

This study established adiabatic scaling laws for direct-drive implosions of solid spheres using three-step pulse lasers. Although implosion is a complex phenomenon involving entropy generation through shock waves, thermal conduction, and radiative transport, the adiabatic approximation is assumed to hold for differences between similar implosion scenarios. Numerous one-dimensional numerical experiments confirmed the validity of Eq. (6), which describes the relationship between density at maximum compression and confinement time. These results suggest that measuring the timescale required for plasma expansion could enable accurate density prediction.

Acknowledgments

This work was partially supported by JSPS KAKENHI Grant Number JP24K17030 and the Institute of Laser Engineering, The University of Osaka through Joint Research Project No. “2025B2-017SHIROTO”. During the preparation of this work, the author used “DeepL” in order to improve the language. After using this tool, the author reviewed and edited the content as needed and takes full responsibility for the content of the publication.

[1] S. Fujioka *et al.*, Phys. Plasmas **23**, 056308 (2016).
[2] H. Sawada *et al.*, Appl. Phys. Lett. **108**, 254101 (2016).
[3] S. Sakata *et al.*, Nat. Commum. **9**, 3937 (2018).
[4] T. Gong *et al.*, Nat. Commum. **10**, 5614 (2019).
[5] R. Takizawa *et al.*, Phys. Rev. Res. **7**, 023081 (2025).
[6] R.E. Kidder, Nucl. Fusion **14**, 53 (1974).
[7] H. Nagatomo *et al.*, Nucl. Fusion **59**, 106055 (2019).
[8] H. Nagatomo *et al.*, Nucl. Fusion **61**, 126032 (2021).
[9] H. Nagatomo *et al.*, Nucl. Fusion **64**, 106019 (2024).
[10] N. Ohnishi, High Energ. Dens. Phys. **8**, 341 (2012).
[11] L. Spitzer and R. Härm, Phys. Rev. **89**, 977 (1953).
[12] G.N. Minerbo, J. Quant. Spectrosc. Radiat. Transf. **20**, 541 (1978).
[13] H. Takabe and T. Nishikawa, J. Quant. Spectrosc. Radiat. Transf. **51**, 379 (1994).
[14] R.D. Cowan, *The Theory of Atomic Structure and Spectra*, (University of California, Berkeley, 1981).
[15] R.M. More *et al.*, Phys. Fluids **31**, 3059 (1988).